On the Capacity of Underwater Optical Wireless Communication Systems

Yue Rong
School EECMS, Curtin University
Bentley, WA, Australia
y.rong@curtin.edu.au

Sven Nordholm
School EECMS, Curtin University
Bentley, WA, Australia
s.nordholm@curtin.edu.au

Alec Duncan
CMST, Curtin University
Bentley, WA, Australia
a.j.duncan@curtin.edu.au

2021 Fifth Underwater Communications and Networking Conference (UComms) | 978-1-7281-9315-1/21/$31.00 ©2021 IEEE | DOI: 10.1109/UCOMMS50339.2021.9598156

***Abstract*—In this paper, we first analyze the factors that affect the capacity of underwater optical wireless communication (UOWC) systems through deriving a new tight capacity upper-bound. We find that the system capacity depends on the light wavelength in a complicated manner. Then we compare UOWC with the underwater acoustic communication (UAC) technology in terms of channel capacity, communication range, and energy efficiency. We show that UOWC requires a much lower energy-per-bit than UAC for short range communication. Finally, we study the multi-hop communication technique to extend the range of UOWC. The optimal number of hops is derived taking into account the cost of deploying relay nodes. Our study provides useful guidelines in designing a hybrid underwater acoustic/optical communication system which can achieve an increased range-rate product for underwater wireless communication.**

***Index Terms*—Underwater optical wireless communication, underwater acoustic communication**

I. Introduction

Wireless information transmission through the underwater medium is traditionally implemented through underwater acoustic communication (UAC). A major advantage of UAC is that long range communication (several tens of kilometers) can be achieved. However, UAC has a low data rate (kbits/s) due to the limited bandwidth of the underwater acoustic channel [1]. Moreover, UAC has a long latency due to the slow propagation of acoustic wave in water. Recently, underwater optical wireless communication (UOWC) attracted much attention, as it can support a much higher data rate (Mbits/s) and has a much shorter latency compared with UAC systems. As a drawback, the range of UOWC is usually shorter (up to 100 m in many environments) compared with UAC [2].

In this paper, we first derive a new tight upper-bound of the capacity of UOWC systems. Based on this upper-bound, we analyze the factors which affect the capacity of UOWC, including environmental factors and system design parameters. Compared with laser, light emitting diodes (LEDs) are less expensive and more robust against transceiver misalignment. Moreover, the LED technology has improved significantly in recent years. Thus, in this paper, we focus on LED as the UOWC transmitter. We find that the system capacity depends on the light wavelength in a complicated manner through various parameters. Then we provide a detailed comparison of the UOWC and UAC technologies in terms of channel capacity, communication range, and energy efficiency. We show that UOWC requires a much lower energy-per-bit than UAC for short range communication. Such comparison provides useful guidelines in designing a hybrid underwater acoustic/optical communication system to overcome the drawbacks of one physical communication technology through the use of a complementary technology. Thirdly, we show that the range of UOWC can be efficiently extended through the multi-hop communication technique. The optimal number of hops is derived taking into account the cost of deploying relay nodes.

The rest of this paper is organized as follows. In Section II we study the impact of various parameters on the capacity of UOWC. In Section III, we compare the performance of UOWC and UAC systems. Multi-hop UOWC systems are investigated in Section IV. Conclusions are drawn in Section V.

This research was supported by the Defence Science Centre, an initiative of the State Government of Western Australia.

II. Capacity of UOWC Systems

Based on [2] and [3], the capacity of a UOWC system is given by

$$C = B\log_2\left(1+\frac{i_s^2}{i_n^2}\right) \tag{1}$$

where B is the system bandwidth, i_s is the current at the receiver generated by the incident light-of-interest, and i_n is the background noise current at the receiver photodiode (PD) as

$$i_s = SP_r, \quad i_n = i_{n,j} + i_{n,s}. \tag{2}$$

Here P_r is the optical power from the light-of-interest received by the receiver PD,

$$S = \frac{\eta q \lambda}{hv} \tag{3}$$

is the sensitivity (also called responsivity in some works) of the PD, η is the quantum efficiency, $q = 1.6\times10^{-19}$C is the electronic charge, $v = 2.25\times10^{8}$ m/s is the speed of light in water, λ is the wavelength of the light-of-interest, and $h = 6.63\times10^{-34}$ Js is the Planck's constant.

In (2), $i_{n,j}$ is the Johnson-Nyquist noise (thermal noise) originating from the feedback resistor in the receiver amplifier circuit and $i_{n,s}$ is the shot noise given respectively by

$$i_{n,j} = \sqrt{4k_BTB/R} \tag{4}$$

$$i_{n,s} = \sqrt{2q(i_d+i_s+i_a)B} \tag{5}$$

where $k_B = 1.38\times10^{-23}$ J/K is the Boltzmann constant, T is the temperature in Kelvin, R is the resistance of the feedback resistor, i_d is the receiver PD dark current, and $i_a = SP_a$ is the current at the receiver caused by the solar and blackbody

radiation. Here, P_a is the received optical power from the solar and blackbody radiation calculated by [2], [4]

$$P_a = \frac{\pi^2 D^2 F_v^2 \int_\Delta (L_a + L_b) d\lambda}{16} \tag{6}$$

where L_a is the upwelling solar spectral radiance, L_b is the blackbody spectral radiance, F_v is the plane angle radian measure of the field of view (FOV) of the receiver, D is the diameter of the receiver PD aperture, and Δ is the optical filter bandwidth. In (6), L_a and L_b are calculated respectively by [4]

$$L_a = \frac{E R_f L_f e^{-c_d d_w}}{\pi} \tag{7}$$

$$L_b = 2hv^2 \alpha \lambda^{-5} (e^{\frac{hv}{\lambda k_B T}} - 1)^{-1} \tag{8}$$

where E is the downwelling solar spectral irradiance, R_f is the underwater reflectance, c_d is the diffuse attenuation coefficient, d_w is the water depth at the receiver, L_f describes the directional dependence of underwater radiance, and α is the radiant absorption factor.

By substituting the expressions of i_s and i_n in (2)-(5) back into (1) we have

$$C = B \log_2 \left(1 + \frac{S^2 P_r^2}{4k_B TB/R + 2q(i_d + SP_r + SP_a)B} \right). \tag{9}$$

We would like to note that the multi-scattering behavior is not considered in (9). Multiple scattering may compensate the path loss overestimated by the simple model in our paper [5]. We will consider the multi-scattering channel model in our future work. The received optical power P_r is calculated as [6]

$$P_r = \frac{P_s A_r e^{-c_l d} \cos\beta}{A_s} \tag{10}$$

where c_l is the light attenuation coefficient, d is the transmitter-receiver distance, β is the receiver's inclination angle with respect to the direction of the light-of-interest, $P_s = \eta_e P_e$ is the transmit optical power, P_e is the input electrical power, η_e is the electrical power to optical power conversion efficiency, A_r is the effective receive area of the receiver PD, and A_s is the beam area at the distance of d given respectively by

$$A_r = \pi D^2/4, \quad A_s = \pi (d \tan\theta)^2. \tag{11}$$

Here θ is the half angle of transmitter beam width [6]. By substituting (11) back into (10), we obtain

$$P_r = \frac{\eta_e P_e D^2 e^{-c_l d} \cos\beta}{4d^2 \tan^2\theta}. \tag{12}$$

In the following, we derive an upper-bound of (9) which helps to shed light on the dependence of the capacity of a UOWC system on various environmental and system design parameters. When P_r is small compared with P_a, which may occur in clean shallow water environment with strong solar radiation [7], (9) can be upper-bounded by setting $P_r = 0$ in its denominator as

$$C = B \log_2 (1 + g P_e^2 e^{-2c_l d} d^{-4}) \tag{13}$$

where

$$g = \frac{S^2 \eta_e^2 D^4 \cos^2\beta}{16 \tan^4\theta (4k_B TB/R + 2q(i_d + SP_a)B)} \tag{14}$$

is obtained by substituting (12) into P_r in the numerator of (9).

It can be easily seen from (13) and (14) that C increases with P_e, η_e, D, R, S, and decreases with d, β, θ, T, i_d and P_a. These parameters (except for P_a which largely depends on the solar radiation) can be properly chosen to increase C. We also observe from (6), (7), and (14) that the capacity of a UOWC system increases with d_w, thanks to reduced solar radiation power with increasing water depth. From (3), we can see that S depends on λ and η. It is shown in [6] that in general η increases with λ, thus S increases with λ. However, the overall dependence of C on the wavelength is rather complicated. Firstly, the decreasing rate of P_r in (12) with respect to d largely depends on c_l, which can be quite different at various λ. Secondly, it is shown [2] that in clean ocean water, there is roughly $c_d = c_l/3$, and from (6), (7), and (14) an increasing c_l also reduces P_a. Thirdly, the solar spectral irradiance E changes with λ. According to Fig. 7 of [4], E is reduced to zero (i.e., no solar noise) at sea level for $\lambda < 300$ nm.

It is shown [8] that $c_l = a_l + b_l$, where a_l and b_l are the absorption coefficient and the scattering coefficient of light in water, respectively. Both a_l and b_l strongly depend on wavelength and environment [8]. In clean ocean water, a_l is smallest at deep blue light ($\lambda = 400$ nm) among all visible light, while with increasing turbidity of water, the minimal a_l shifts towards green and yellow light ($\lambda = 550 \sim 600$ nm). On the other hand, b_l decreases with λ in the visible light range. In general, a suitable wavelength should be chosen by jointly considering the receiver PD sensitivity, light attenuation, and the solar spectral irradiance.

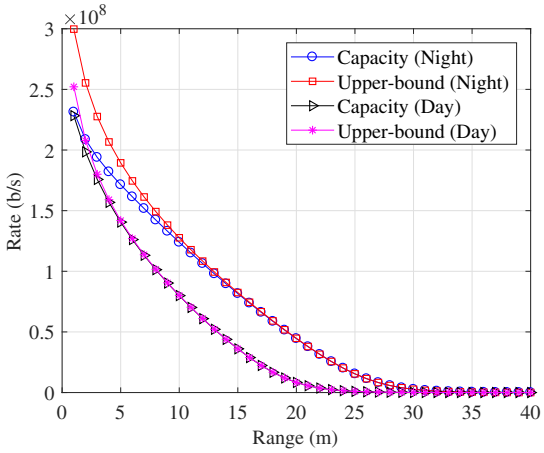

Fig. 1. UOWC system capacity versus range.

Fig. 1 shows the capacity of a UOWC system (9) and its upper-bound (13) during daytime and at night ($E = 0$). The system and environmental parameters used to obtain the results in Fig. 1 are listed in Table I, where the parameters of the receiver PD are taken from the Osram BPW34B silicon

PIN photodiode with enhanced blue sensitivity. It can be seen from Fig. 1 that due to the absence of solar noise, the communication range is increased by 5 m at night. We can also observe that the upper-bounds are quite tight, particulary after the 3 m range during daytime, and after the 10 m range at night. Note that choosing $\Delta = 200$ nm gives a pessimistic estimation of the capacity of a UOWC system during daytime.

TABLE I
UOWC SYSTEM PARAMETERS

Wavelength	λ	400 nm
Input electrical power	P_e	10 W
Bandwidth	B	10 MHz
Light attenuation coefficient	c_l	0.151
Power conversion efficiency	η_e	0.7
Receiver PD sensitivity	S	0.2 A/W
Diameter of the receiver PD	D	1 cm
Receiver PD dark current	i_d	2 nA
Optical filter bandwidth	Δ	200 nm
Receiver inclination angle	β	10°
Half angle of transmitter beam width	θ	45°
Plane angle measure of receiver FOV	F_v	30°
Feedback resistor	R	200 kΩ
Temperature	T	300 K
Water depth	d_w	10 m
Directional dependence of underwater radiance	L_f	2.9
Underwater reflectance	R_f	1.25%
Radiant absorption factor	α	0.5

III. COMPARISON BETWEEN UOWC AND UAC

In this section, we compare the performance of the two major underwater wireless communication systems in terms of their capacity and energy efficiency. The path loss of the underwater acoustic channel over a distance of d is $d^k a_f^d$ [1], where k is the spreading factor and a_f is the channel absorption coefficient. The capacity of UAC systems has been studied in [1] using the Thorp's formula on a_f [9] as

$$a_f = \frac{0.11 f^2}{1+f^2} + \frac{44 f^2}{4100+f^2} + 2.75 \cdot 10^{-4} f^2 + 0.003$$

where f is frequency in kHz and a_f is in dB/km. The noise model of UAC systems is presented in [10] as

$$\begin{aligned} N_t &= 17 - 30 \log_{10} f \\ N_s &= 40 + 20(s - 0.5) + 26 \log_{10} f - 60 \log_{10}(f + 0.03) \\ N_w &= 50 + 7.5\sqrt{w} + 20 \log_{10} f - 40 \log_{10}(f + 0.4) \\ N_{th} &= -15 + 20 \log_{10} f \end{aligned}$$

where N_t, N_s, N_w, and N_{th} are the power spectral density (in dB re μPa per Hz) of the turbulence, shipping, waves, and thermal noise, respectively, s is the shipping activity factor, and w is the wind speed in m/s.

Fig. 2 shows the comparison of the capacity of UOWC and UAC systems. The parameters of the UOWC system are adopted from Table I for the clean ocean environment, with $c_l = 0.298$ for the coastal ocean environment, and $c_l = 2.19$ for the turbid harbor conditions. For the acoustic systems, we study the rate of both a high frequency (HF) and a low frequency (LF) system, whose parameters are listed in Table II. It can be seen that for short distances, the optical system achieves a higher rate. However, due to a higher channel path loss, the rate of the optical systems decreases much faster when the range increases compared with the acoustic systems.

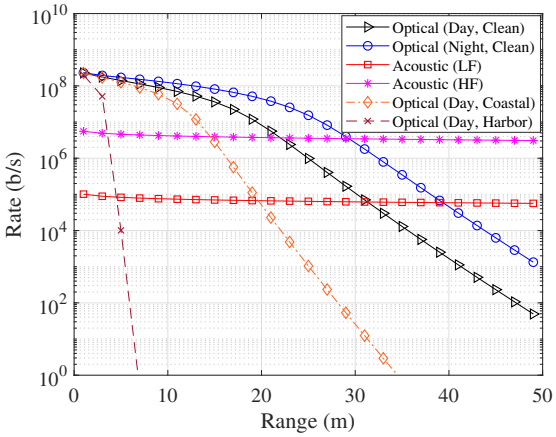

Fig. 2. Capacity comparison of UOWC and UAC systems.

TABLE II
UAC SYSTEM PARAMETERS

Carrier frequency	f_c	LF: 12 kHz, HF: 300 kHz
Bandwidth	B	LF: 4 kHz, HF: 200 kHz
Spreading factor	k	2
Shipping activity factor	s	1
Wind speed	w	10 m/s

Fig. 3 shows the comparison of the two systems in terms of energy-per-bit calculated by P_e/C. It can be seen that the optical systems have a much lower energy consumption at short range than the acoustic systems. We can see from Figs. 2 and 3 that compared with the clean ocean environment, the crossover between the optical and acoustic systems occurs at a shorter range in coastal ocean and turbid harbor environments. The results in Figs. 2 and 3 motivate a hybrid underwater acoustic and optical communication system which can achieve an increased range-rate product over the entire range.

IV. MULTI-HOP UOWC LINK

It can be seen from Fig. 3 that UOWC systems may consume a large amount of energy when the communication range increases. To reduce the amount of transmission power and extend the range of UOWC systems, we can introduce relay nodes between the transmitter and receiver, such that the communication between the transmitter and the receiver is completed in multiple hops. For a given signal-to-noise ratio (SNR) $\rho = i_s^2/i_n^2$, let us define

$$a = \rho(4k_B T B/R + 2q(i_d + SP_a)B)/S^2, \quad b = 2qB\rho/S.$$

From (9), the power P_r required to achieve ρ is given by

$$P_r = \frac{b + \sqrt{b^2 + 4a}}{2}. \tag{15}$$

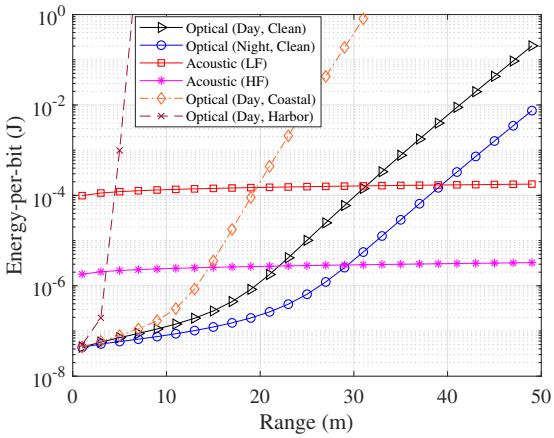

Fig. 3. Energy-per-bit comparison of UOWC and UAC systems.

By substituting (15) back into (12), we obtain

$$P_e = \gamma d^2 e^{c_l d} \tag{16}$$

where

$$\gamma = \frac{2\tan^2\theta(b+\sqrt{b^2+4a})}{\eta D^2 \cos\beta}.$$

Assuming that the relay nodes are located on the line between the transmitter and receiver with equal distance, then the distance of each hop is $d_r = d/N$. Based on (16), the total transmission power required over N hops is

$$P_t = N\gamma d_r^2 e^{c_l d_r} = \frac{\gamma d^2}{N} e^{c_l d/N}.$$

Let us introduce P_0 as the cost of deploying a relay node in terms of power consumption (e.g. the circuit power). Then the overall objective function is

$$P_f = P_t + (N-1)P_0 = \frac{\gamma d^2}{N} e^{c_l d/N} + (N-1)P_0. \tag{17}$$

By setting the derivative of (17) with respect to N to zero, we obtain the following nonlinear equation

$$\frac{\gamma d^2}{N^2} e^{c_l d/N} \left(1 + \frac{c_l d}{N}\right) = P_0. \tag{18}$$

Considering that N is an integer, we find that the optimal number of hops N^* minimizing (17) is either $N^* = \lfloor N_o \rfloor$ or $N^* = \lceil N_o \rceil$, where $\lfloor\cdot\rfloor$ and $\lceil\cdot\rceil$ are the floor and ceiling functions, respectively, and N_o is the solution of (18). We can see from (18) that N_o increases with d and decreases with P_0. Considering that the relay nodes operate in the practical half-duplex mode, the system capacity becomes $C/2$. Thus, the energy-per-bit of an N-hop UOWC system is given by

$$\frac{2P_f}{C} = \frac{2(\gamma d^2 e^{c_l d/N} + N(N-1)P_0)}{NB\log_2(1+\rho)}. \tag{19}$$

Fig. 4 shows the overall system power consumption P_f in (17) versus the number of hops at various ranges with $P_0 = 1$ W. The other parameters are set according to Table I. It can be seen that the system power consumption can be greatly reduced by deploying multiple hops. For a range of 300 m, a power saving of 30 dB can be obtained through a 3-hop UOWC system. We also observe from Fig. 4 that the optimal number of hops N^* increases with the communication range.

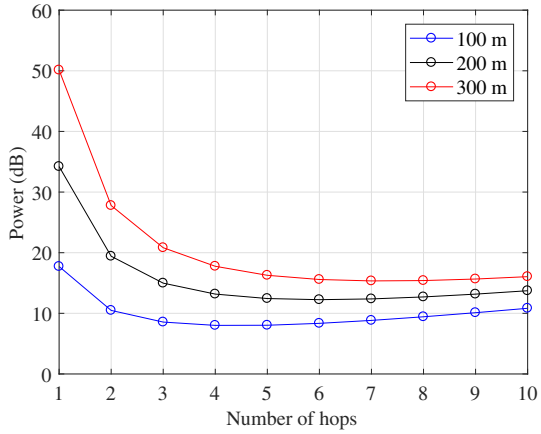

Fig. 4. System power required by multi-hop UOWC.

A potential drawback of multi-hop UOWC systems is the end-to-end delay for a packet to be transmitted from the transmitter to the receiver. Assuming that there are L bits in a packet, the delay of one packet is $d/v + NL/C$. This delay needs to be considered in practical UOWC system design.

V. Conclusions

We have compared the performance of UOWC and UAC systems in terms of data rate and energy efficiency. A multi-hop system has been investigated to extend the range of UOWC. In the future, we shall investigate a hybrid optical/acoustic system to increase the range and rate of underwater wireless communication.

References

[1] M. Stojanovic, "On the relationship between capacity and distance in an underwater acoustic communication channel," in *Proc. WUWNet*, Los Angeles, CA, USA, Sep. 25, 2006.

[2] J. W. Giles and I. N. Bankman, "Underwater optical communications systems. Part 2: Basic design considerations," in *Proc. IEEE Military Commun. Conf.*, vol. 3. 2005, pp. 1700-1705.

[3] D. Anguita, D. Brizzolara, G. Parodi, and Q. Hu, "Optical wireless underwater communication for AUV: Preliminary simulation and experimental results," in *Proc. IEEE/OES Oceans*, Santander, Spain, Jun. 2011.

[4] N. S. Kopeika and J. Bordogna, "Background noise in optical communication systems," *Proc. IEEE*, vol. 58, pp. 1571-1577, Oct. 1970.

[5] H. Zhang and Y. Dong, "General stochastic channel model and performance evaluation for underwater wireless optical links," *IEEE Trans. Wireless Commun.*, vol. 15, pp. 1161-1173, Feb. 2016.

[6] J. Sticklus, P. Hoeher, and R. Röttgers, "Optical underwater communication: The potential of using converted green LEDs in coastal waters," *IEEE J. Oceanic Engineering*, vol. 44, pp. 535-547, Apr. 2019.

[7] F. Campagnaro, M. Calore, P. Casari, V. S. Calzado, G. Cupertino, C. Moriconi, M. Zorzi, "Measurement-based simulation of underwater optical networks," in *Proc. IEEE/OES Oceans*, Aberdeen, U.K., Jun. 2017.

[8] C. D. Mobley, *Light and Water: Radiative Transfer in Natural Waters.* London, U.K.: Academic Press, 1994.

[9] L. Berkhovskikh and Y. Lysanov, *Fundamentals of Ocean Acoustics.* New York: Springer, 1982.

[10] R. Coates, *Underwater Acoustic Systems.* New York: Wiley, 1989.